THE JOURNAL OF BIOLOGICAL CHEMISTRY
Vol. 274, No. 39, Issue of September 24, pp. 27407–27414, 1999

Printed in U.S.A.

Neosynthesis and Activation of Rho by *Escherichia coli* Cytotoxic Necrotizing Factor (CNF1) Reverse Cytopathic Effects of ADP-ribosylated Rho*

(Received for publication, May 24, 1999)

Holger Barth‡, Claudia Olenik‡, Peter Sehr, Gudula Schmidt, Klaus Aktories§, and Dieter K. Meyer¶

From the Institut für Pharmakologie und Toxikologie der Albert-Ludwigs-Universität Freiburg, Hermann-Herder-Strasse 5, D-79104 Freiburg, Germany

Clostridium botulinum **exoenzyme C3 inactivates the small GTPase Rho by ADP-ribosylation. We used a C3 fusion toxin (C2IN-C3) with high cell accessibility to study the kinetics of Rho inactivation by ADP-ribosylation. In primary cultures of rat astroglial cells and Chinese hamster ovary cells, C2IN-C3 induced the complete ADP-ribosylation of RhoA and concomitantly the disassembly of stress fibers within 3 h. Removal of C2IN-C3 from the medium caused the recovery of stress fibers and normal cell morphology within 4 h. The regeneration was preceded by the appearance of non-ADP-ribosylated RhoA. Recovery of cell morphology was blocked by the proteasome inhibitor lactacystin and by the translation inhibitors cycloheximide and puromycin, indicating that intracellular degradation of the C3 fusion toxin and the neosynthesis of Rho were required for reversal of cell morphology.** ***Escherichia coli*** **cytotoxic necrotizing factor CNF1, which activates Rho by deamidation of Gln^{63}, caused reconstitution of stress fibers and cell morphology in C2IN-C3-treated cells within 30–60 min. The effect of CNF1 was independent of RhoA neosynthesis and occurred in the presence of completely ADP-ribosylated RhoA. The data show three novel findings; 1) the cytopathic effects of ADP-ribosylation of Rho are rapidly reversed by neosynthesis of Rho, 2) CNF1-induced deamidation activates ADP-ribosylated Rho, and 3) inhibition of Rho activation but not inhibition of Rho-effector interaction is a major mechanism underlying inhibition of cellular functions of Rho by ADP-ribosylation.**

The low molecular mass GTPases of the Rho family (Rho, Rac, and Cdc42) play key roles in the control of the actin cytoskeleton (1). In several cell lines, activation of RhoA induces formation of stress fibers and focal adhesions (2), whereas Rac and Cdc42 cause the formation of lamellipodia and filopodia, respectively (2–4). Moreover, Rho GTPases act as molecular switches in various signaling processes (5) including secretion (6), phagocytosis (7), endocytosis (8, 9), cell cycle progression (10), transcriptional activation (11), and transformation (12).

Rho proteins are the eukaryotic targets of various bacterial toxins that inactivate or activate the GTPases by covalent modification (13). Whereas the large clostridial cytotoxins (*e.g. Clostridium difficile* toxins A and B) inactivate Rho GTPases by glucosylation at Thr$^{35/37}$ (14, 15), the cytotoxic necrotizing factor from *Escherichia coli* (*E. coli* CNF1) activates the GTPases by deamidation of Gln$^{61/63}$ (16–18). Moreover, RhoA, -B, and -C but not Rac1 and Cdc42 are substrates of exoenzyme C3 from *Clostridium botulinum* (19–21) or *Clostridium limosum* (22), which inactivates the GTPases by ADP-ribosylation at Asn^{41} (22). C3 exoenzyme in particular is widely used as a cell biological tool to study the functions of Rho (23).

Inasmuch as C3 exoenzyme appears to enter cells via nonspecific pinocytosis, its cell accessibility is poor (24). Recently, we constructed a C3 fusion toxin, which enters cells by using the binary *C. botulinum* C2 toxin as a carrier (25). The actin-ADP-ribosylating C2 toxin consists of the ~80-kDa binding component (C2II) and the 49-kDa enzymatic component (C2I) (26–28). Both C2 components are separate proteins which assemble at the cell surface after C2II has bound to an unknown receptor. The C3 fusion toxin (C2IN-C3) contains the N-terminal domain (amino acid residues 1- 225) of C2I (C2IN), which has no enzyme activity but binds to the C2II component and is sufficient for translocation of C2I into the cytosol. In contrast to C3 exoenzyme, the C2IN-C3 fusion toxin enters cells readily and causes the depolymerization of stress fibers at low toxin concentration within a few hours (25). Thus, C2IN-C3 allows the study of the kinetics of the cellular intoxication process in more detail.

Here we report that the cytopathic effects of the C2IN-C3 fusion toxin are rapidly reversed after removal of the toxin. Reversal of the C3-induced alterations of the cytoskeleton is caused by rapid degradation of the toxin and by resynthesis of Rho. Moreover, we show that the Rho-deamidating toxin CNF1 reverses the effects of C2IN-C3 most likely by reactivating ADP-ribosylated Rho. The data provide new insights into the mechanism of the action of C3 and indicate that ADP-ribosylated Rho is still able to interact with effectors and to activate their targets.

EXPERIMENTAL PROCEDURES

Materials and Chemicals—Cell culture medium was purchased from Biochrom (Berlin, Germany), fetal calf serum from PAN Systems (Aidenbach, Germany) and Life Technologies, Inc. (Heidelberg, Germany), and cell culture materials from Falcon (Heidelberg, Germany). Lab-Tec chamber slides were from Permanox (Nunc, Germany). The C2II binding component from the *C. botulinum* C2 toxin was purified and activated with trypsin as described (26, 29). The C2IN-C3 fusion toxin (25)

* This work was supported by Deutsche Forschungsgemeinschaft Sonderforschungsbereich 388 and 505/B4. The costs of publication of this article were defrayed in part by the payment of page charges. This article must therefore be hereby marked "*advertisement*" in accordance with 18 U.S.C. Section 1734 solely to indicate this fact.

‡Both authors contributed equally to this work.
§ To whom correspondence may be addressed. Tel.: 49-761-2035301; Fax: 49-761-2035311; E-mail: aktories@uni-freiburg.de.
¶ To whom correspondence may be addressed. Tel.: 49-761-2035327; Fax: 49-761-2035326; E-mail: meyerdk@uni-freiburg.de.

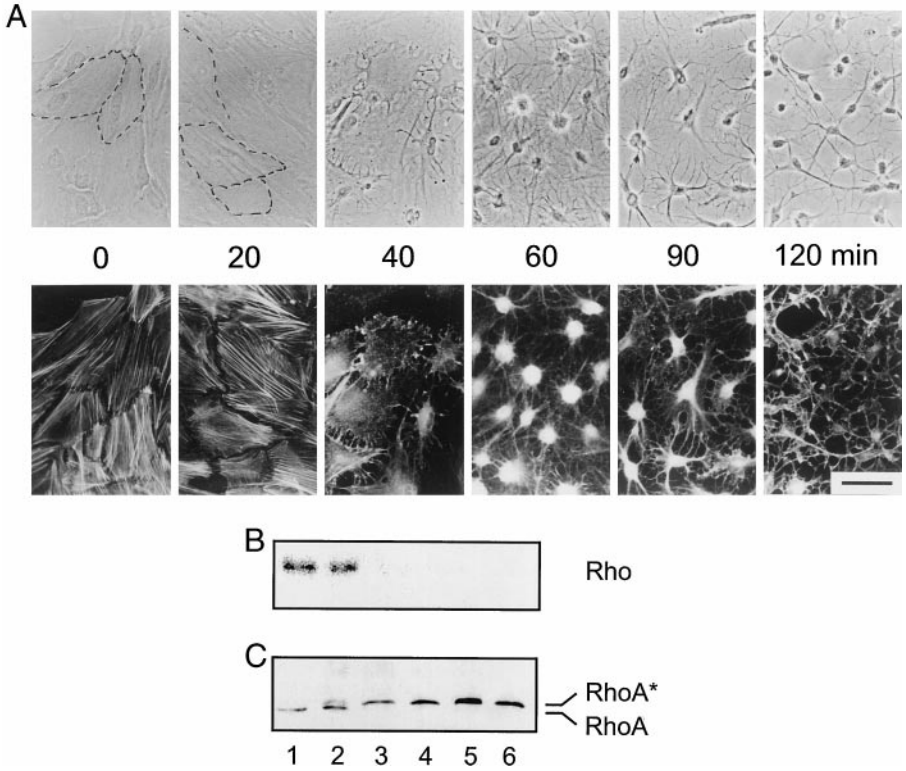

FIG. 1. **Time course of the effects of C2IN-C3/C2II on astroglial cells in primary culture.** *A*, toxin effects are shown on cells morphology and the actin cytoskeleton. Cells grown on Lab-Tec chamber slides were incubated with C2IN-C3 (100 ng/ml) and C2II (200 ng/ml) in the medium. At the indicated times, cells were fixed and the actin filaments were stained with rhodamine-phalloidin. Some flat polygonal cells are visualized by *dashed lines*. *Upper part*, phase contrast pictures; *lower part*, rhodamine-phalloidin staining of the actin filaments of the respective cells. *Bar* = 50 μm. *B*, ADP-ribosylation of Rho by C2IN-C3/C2II treatment of astroglial cells. Cells were treated without toxin (*lane 1*) or with C2IN-C3/C2II for 20 min (*lane 2*), 40 min (*lane 3*), 60 min (*lane 4*), 90 min (*lane 5*), and 120 min (*lane 6*), respectively. After toxin treatment, the cells were lysed and lysate proteins (100 μg) were subjected to an *in vitro* [^{32}P]ADP-ribosylation assay with C3 as described under "Experimental Procedures." Labeled proteins were detected by SDS-PAGE and autoradiography. *C*, anti-RhoA immunoblot analysis of 100 μg of the same lysates described above. ADP-ribosylated RhoA is indicated by an *asterisk*.

and CNF1 (16) were purified as recombinant GST[1] fusion proteins as described. The pGEX-LBC construct was kindly donated by Denniz Toksoz, Harvard Medical School, Boston, MA (30). LBC was purified as a recombinant GST fusion protein. 2′-(3′)-*O*-(*N*-Methylanthraniloyl) guanosine 5′-diphosphate (mant-GDP) was prepared as described (31). The pGEX2T vector (included in the GST Gene Fusion System) and glutathione-Sepharose 4B were from Amersham Pharmacia Biotech (Uppsala, Sweden). Anti-RhoA-antibody and horseradish peroxidase-coupled anti-mouse antibody were from Santa Cruz (Heidelberg, Germany). Rhodamine-phalloidin, puromycin and cycloheximide were purchased from Sigma (Deisenhofen, Germany). [^{32}P]NAD (30 Ci/mmol) was from NEN Life Science Products (Bad Homburg, Germany). Nylon membrane for RNA blotting, the DIG *in vitro* transcription kit, and the DIG DNA labeling and detection kit were from Roche Molecular Biochemicals (Mannheim, Germany). Lactacystin was from Calbiochem (Bad Soden, Germany).

Cell Culture—CHO-K1 cells were cultivated in tissue culture flasks at 37 °C and 5% CO_2 in Ham's F-12/Dulbecco's modified Eagle's medium (1:1) containing 5% heat-inactivated (30 min, 56 °C) fetal calf serum, 2 mM L-glutamate, 100 units/ml penicillin, and 100 μg/ml streptomycin. Cells were routinely trypsinized and reseeded twice a week. Primary cultures of rat astroglial cells were set up as described previously (32, 33). For cytotoxicity and regeneration assays, subconfluent cells (about 10^5 to 5×10^5 cells/cm^2) in 3-cm plates containing coverslips or cells growing on Lab-Tec chamber slides were treated for different times with 200 ng/ml activated C2II together with 100 ng/ml C2IN-C3. CNF1 was used in a final concentration of 300 ng/ml medium. For regeneration assays cells were treated with the respective toxin for 3 h; then the cells were washed 5 times with prewarmed medium, new medium without any toxin was added, and the cells were incubated at 37 °C.

Actin Staining—For fluorescence staining of F-actin, cells were fixed in 4% paraformaldehyde containing 0.1% Triton X-100 for 30 min. Thereafter, cells were briefly washed and incubated for 30 min with rhodamine-phalloidin (600 ng/ml).

ADP-ribosylation Assay of Rho—Cells were treated with the respective toxins as indicated. After incubation they were washed with cold PBS, harvested in 400 μl of cold lysis buffer (2 mM $MgCl_2$, 0.1 mM phenylmethylsulfonyl fluoride, 20 μg/ml leupeptin, 80 μg/ml benzamidine in 50 mM HEPES, pH 7.4) and sonicated. Aliquots (100 μg of protein) of the lysate were incubated with [^{32}P]NAD and 50 ng of C2IN-C3 fusion toxin at 37 °C for 30 min, Laemmli buffer was added, the samples were heated for 3 min at 95 °C and run on sodium dodecyl sulfate-polyacrylamide gel electrophoresis (SDS-PAGE). [^{32}P]ADP-ribosylated proteins were detected by autoradiography with a PhosphorImager from Molecular Dynamics (Krefeld, Germany).

SDS-PAGE and Western Blotting —SDS-PAGE was performed according to Laemmli (34). For immunoblot analysis, the proteins were transferred onto a nitrocellulose membrane. The membrane was blocked for 30 min with 5% nonfat dry milk in PBS containing 0.05% Tween 20 (PBS-T) and the proteins were probed with anti-RhoA antibody (mouse, 1:2000 in PBS-T). After washing with PBS-T, the blot was incubated for 1 h with an anti-mouse antibody coupled to horseradish peroxidase (1:2000 in PBS-T). The membrane was washed again, and proteins were visualized using the ECL system according to the manufacturer's instructions.

Extraction and Filter Hybridization of RNA—Total RNA was extracted by the guanidine hydrochloride method (35). Seven-μg aliquots were separated by denaturing gel electrophoresis (1.25% formaldehyde agarose gels; running buffer was 20 mM MOPS, 8 mM NaAc, and 1 mM EDTA) and electroblotted onto a nylon membrane. The following nonradioactive DIG filter hybridization and detection of RhoA mRNA was performed as described previously (36, 37).

Fluorescence Assay for Nucleotide Exchange—All measurements were done on a LS50B spectrofluorometer from Perkin Elmer at 37 °C. First RhoA was loaded with the fluorescent nucleotide mant-GDP by incubating 0.5 μM GTPase with 2 μM mant-GDP in buffer C (10 mM triethanolamine, pH 7.5, 150 mM NaCl, 2 mM $MgCl_2$) for 1 h. Thereafter, the exchange of Rho-bound mant-GDP for GTP was initiated by adding 100 μM GTP and 0–20 μM LBC. The exchange of Rho-bound fluorescent mant-GDP for GTP was monitored by the decrease in fluorescence intensity upon the release of mant-GDP from RhoA. Exciting of the mant-fluorophor was at 357 nm; emission was measured at 444 nm. The rate constant for the release of mant-GDP was determined by fitting the experimental curve with a single exponential decay using SigmaPlot (Jandel Scientific).

RESULTS

C2IN-C3 Fusion Toxin Rapidly Disassembles Stress Fibers in Rat Astroglial Cells—In primary cultures of rat astrocytes, C2IN-C3 fusion toxin caused changes in cell shape and destruction of stress fibers. These effects started 40 min after addition

[1] The abbreviations used are: GST, glutathione *S*-transferase; mant-GDP, 2′-(3′)-*O*-(*N*-methylanthraniloyl)guanosine 5′-diphosphate; CHO, Chinese hamster ovary; PBS, phosphate-buffered saline; PBS-T, PBS plus Tween 20; PAGE, polyacrylamide gel electrophoresis; LBC, lymphoid blast crisis oncogene; MOPS, 4-morpholinepropanesulfonic acid.

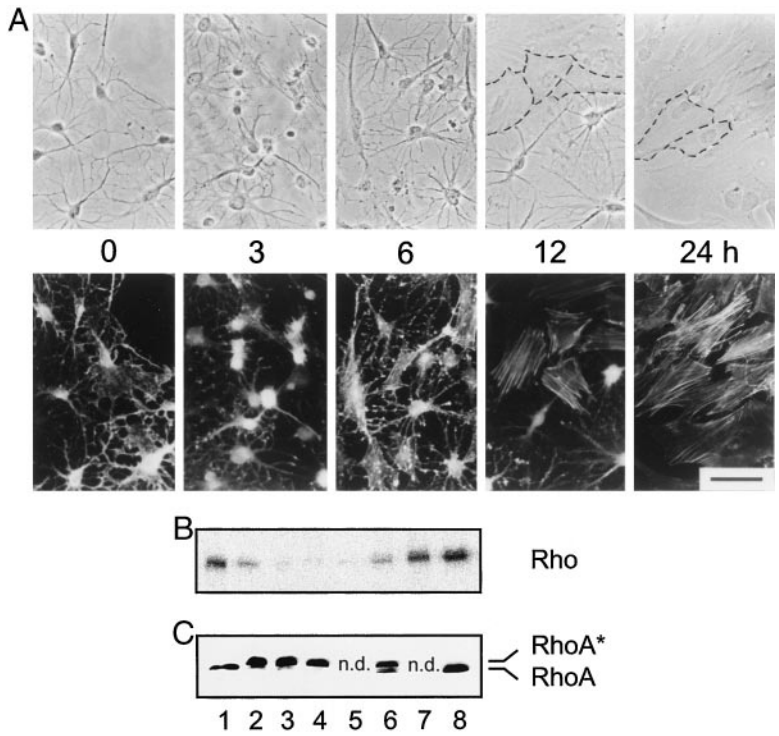

FIG. 2. **Reversal of C3 effects by removal of C2IN-C3/C2II from the medium.** *A*, destruction of actin filaments induced by C2IN-C3 is reversible in astroglial cells in primary culture. Cells growing on Lab-Tec chamber slides were treated for 2 h with 100 ng/ml C2IN-C3 and 200 ng/ml C2II at 37 °C. Then the medium was removed, and cells were washed and incubated without toxin for up to 24 h. Immediately (0 h) or after 3, 6, 12, and 24 h, cells were fixed and stained with rhodamine-phalloidin. Some flat polygonal cells are visualized by *dashed lines*. The *upper part* shows the phase contrast pictures; *lower part* shows the staining of actin filaments of respective cells. *Bar* = 50 μm. *B* and *C*, analysis of ADP-ribosylation of Rho in astroglial cells after treatment with C2IN-C3/C2II and subsequent removal of the toxin from the medium. Cells were treated as described above. Then the medium was removed, and cells were washed and incubated without toxin. At the indicated times, the cells were lysed. Aliquots of the cell lysate protein were analyzed for [^{32}P]ADP-ribosylation of Rho in the ADP-ribosylation assay with C3 transferase, SDS-PAGE, and subsequent autoradiography (*B*). An anti-RhoA immunoblot of the same lysates is shown in *C*. *Lane 1*, control cells; *lane 2*, 1-h incubation with C2IN-C3/C2II; *lane 3*, 2-h incubation with C2IN-C3/C2II; *lane 4*, 6-h incubation with C2IN-C3/C2II; *lane 5*, 24-h incubation with C2IN-C3/C2II; *lane 6*, 2-h incubation with C2IN-C3/C2II followed by a 4-h incubation in fresh medium; *lane 7*, 2-h incubation with C2IN-C3/C2II followed by a 10-h incubation in fresh medium; *lane 8*, 2-h incubation with C2IN-C3/C2II followed by a 24-h incubation in fresh medium. ADP-ribosylated RhoA is indicated by an *asterisk*; *n.d.*, not done for immunoblot.

of the toxin and were maximal after about 2 h (Fig. 1*A*). By 40–60 min after addition of C3 fusion toxin to intact cells, radioactive [^{32}P]ADP-ribosylation of Rho was no longer observed in the cell lysate, indicating the complete modification of cellular Rho (Fig. 1*B*). The ADP-ribosylation of RhoA was confirmed by anti-RhoA immunoblot analysis (Fig. 1*C*). Twenty minutes after addition of the toxin, a fast moving (unmodified Rho) and a slower moving RhoA band (ADP-ribosylated Rho) were detected by immunoblotting. After 40 min, only the ADP-ribosylated RhoA was observed.

Effects of the C2IN-C3 Fusion Toxin Are Reversible—To test whether the effects of the fusion toxin were reversible, astroglial cells were incubated with the toxin for 3 h. Thereafter, the cells were extensively washed to remove extracellular toxin. Stress fibers reappeared 6 h after removal of the toxin, and the recovery was complete after 24 h (Fig. 2*A*). Reorganization of stress fibers was accompanied by the reappearance of the polygonal cell morphology (Fig. 2*A*). Removal of the toxin rapidly changed the proportion of ADP-ribosylated and non-modified Rho (Fig. 2*B*). Four hours after removal of the toxin, *i.e.* when the cells started to rebuild their stress fibers, a small amount of Rho was [^{32}P]ADP-ribosylated. Its level increased with the duration of toxin withdrawal (Fig. 2*B*). Accordingly, 4 h after removal of the toxin, non-ADP-ribosylated RhoA was detected by anti-RhoA immunoblotting and 24 h after toxin withdrawal only non-ADP-ribosylated RhoA was detected (Fig. 2*C*).

Reversal of the C3 effects was not cell type-specific. In CHO cells or HeLa cells, the C3 fusion toxin disassembled stress fibers within 3 h. Removal of the toxin resulted in the reorganization of stress fibers, adhesion to dish matrix, and restoration of cell morphology. The recovery started 2–3 h after addition of fresh medium (data not shown). Reversal of the cytopathic effects seemed to be specific for the fusion toxin. When CHO cells were treated with 10 μg/ml wild-type *C. limosum* C3 exoenzyme for 24 h to induce the "C3 specific" morphology, cells did not recover after removal of the toxin by medium exchange.

Studies on the Duration of Action of the C2IN-C3 Fusion Toxin—Because the cytopathic effects disappeared rapidly after removal of C2IN-C3 from the medium, we studied whether the toxin was intracellularly degraded by proteases. When CHO cells were treated for 3 h with the fusion toxin and subsequently incubated for 16 h in fresh medium in the presence of the proteosome inhibitor lactacystin, cells did not regain their original morphology. In lysates of these cells, Rho was not radioactively labeled by ADP-ribosylation with [^{32}P]NAD and C3 (Fig. 3*A*, *lane 5*). As expected, only a slowly migrating RhoA band was detected by immunoblotting, indicating the presence of Rho ADP-ribosylated in intact cells (Fig. 3*B*, *lane 5*). Thus, lactacystin prolonged the cellular effects of the C3 fusion toxin.

Studies on the Recovery of RhoA—First, we tested whether recovery of non-ADP-ribosylated Rho was due to cleavage of the ADP-ribose moiety from Rho by a cellular hydrolase activity. CHO cells were treated with the C3 fusion toxin for 2 h and then incubated for 1 h in fresh medium without toxin. Cell lysates were prepared and incubated for 0, 3, and 6 h at 37 °C.

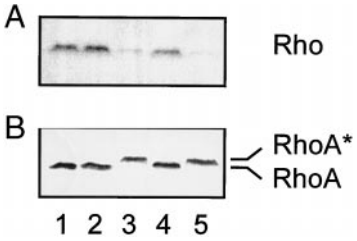

FIG. 3. **Influence of lactacystin on the regeneration of CHO cells after C2IN-C3/C2II treatment.** Cells were incubated for 3 h with 100 ng/ml C2IN-C3 and 200 ng/ml C2II at 37 °C. After removal of the medium and washing, cells were incubated in fresh medium without toxin for an additional 16 h. For inhibition of proteolytic degradation, cells were incubated with lactacystin (30 μM) in the medium. Cells were lysed, and aliquots (50 μg of protein) were [^{32}P]ADP-ribosylated by C3 transferase and analyzed by anti-RhoA immunoblot. *A*, autoradiography of [^{32}P]ADP-ribosylated Rho. *B*, anti-RhoA immunoblot. *Lane 1*, control cells; *lane 2*, 16-h incubation with lactacystin; *lane 3*, 3-h incubation with C2IN-C3/C2II; *lane 4*, 3-h incubation with C2IN-C3/C2II followed by a 16-h incubation in fresh medium; *lane 5*, 3-h incubation with C2IN-C3/C2II followed by a 16-h incubation in fresh medium + lactacystin. ADP-ribosylated RhoA is indicated by an *asterisk*.

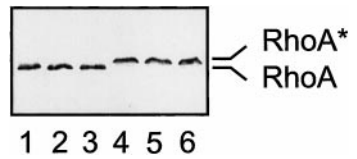

FIG. 4. **Stability of ADP-ribosylated RhoA in lysates of CHO cells.** CHO cells were treated for 3 h with 100 ng/ml C2IN-C3 and 200 ng/ml C2II or for control without toxin at 37 °C. After withdrawal of the medium, cells were washed and incubated in fresh medium without toxin for 1 h. Cells were scraped off into 100 μl of PBS and sonicated, and lysates were incubated in a 37 °C water bath. At the indicated times, aliquots (100 μg of protein) were removed and subjected to SDS-PAGE and subsequent immunoblot analysis with anti-RhoA antibody. *Lane 1*, control 0-h incubated; *lane 2*, control 3-h incubated; *lane 3*, control 6-h incubated; *lane 4*, C2IN-C3 0-h incubated, *lane 5*, C2IN-C3 3-h incubated; *lane 6*, C2IN-C3 6-h incubated.

Thereafter, Rho protein was analyzed by immunoblotting (Fig. 4). Even after incubation of the lysates for 6 h at 37 °C (Fig. 4, *lanes 3* and *6*), a significant proteolysis of RhoA was not detected. Furthermore, in lysates of cells that had been treated with C3 fusion toxin (*lanes 4–6*), the slowly migrating band of ADP-ribosylated RhoA remained stable, while a rapidly migrating RhoA band did not appear. Taking these results together, we were not able to detect hydrolysis of the ADP-ribosylated RhoA in the lysates.

To test whether the reappearance of non-ADP-ribosylated RhoA after toxin withdrawal was due to newly synthesized protein, we blocked protein synthesis with cycloheximide or puromycin. Three hours after addition of the toxin, endogenous Rho was completely ADP-ribosylated (no [^{32}P]ADP-ribosylation, Fig. 5*B*, *lane 2*) and only the slowly moving ADP-ribosylated RhoA band was detected in the immunoblot (Fig. 5*C*, *lane 2*). When cycloheximide or puromycin was present after toxin withdrawal, regeneration of stress fibers (Fig. 5*A*) and [^{32}P]ADP-ribosylation of Rho was not observed (Fig. 5*B*, *lanes 5* and *7*). Moreover, the immunoblot did not show unmodified RhoA (Fig. 5*C*, *lanes 5* and *7*). All these data suggested that protein neosynthesis, not hydrolysis of ADP-ribosylated RhoA, was responsible for the reappearance of non-ADP-ribosylated RhoA.

Northern blot analysis of total RNA extracts from CHO cells was used to investigate whether the rapid neosynthesis was initiated by an increase in RhoA mRNA. Neither addition of the C3 toxin (added for 3 h) nor its removal had any effect on the amount of RhoA mRNA (Fig. 6). Apparently, neosynthesis of

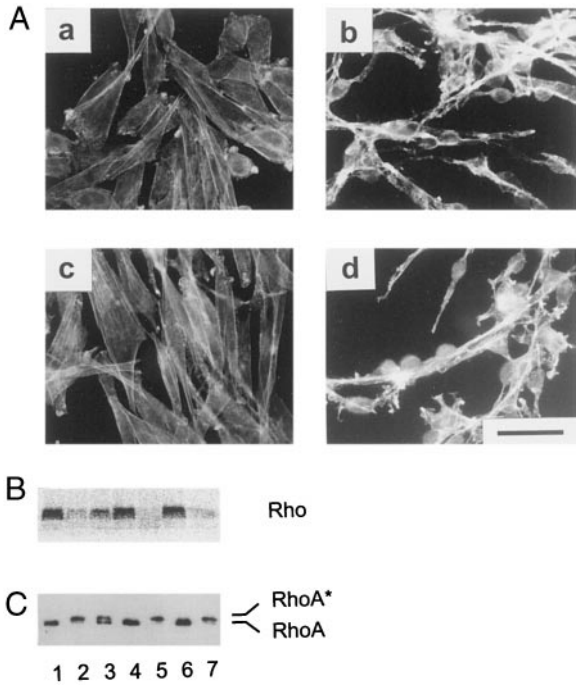

FIG. 5. **Influence of inhibition of protein neosynthesis on the regeneration of CHO cells after C2IN-C3/C2II treatment.** Cells were incubated for 3 h with 100 ng/ml C2I and 200 ng/ml C2II at 37 °C. After removal of the medium and washing, cells were incubated in fresh medium without toxin for another 6 h. For inhibition of protein biosynthesis, cells were incubated with cycloheximide (20 μM) or puromycin (20 μM) in the medium. For control, cells without toxin treatment were grown for 9 h with cycloheximide or puromycin, respectively. At the indicated times, the cells were lysed or fixed for F-actin staining. *A*, rhodamine-phalloidin staining. *a*, control cells; *b*, cells treated for 3 h with C2IN-C3/C2II; *c*, cells incubated for 3 h with C2IN-C3/C2II and subsequently for 6 h in fresh medium; *d*, cells incubated for 3 h with C2IN-C3/C2II and subsequently for 6 h in fresh medium in the presence of cycloheximide. *Bar* = 50 μm. *B*, aliquots of the cell lysates (50 μg of protein) were [^{32}P]ADP-ribosylated by C3 and detected by autoradiography. *C*, anti-RhoA immunoblot. *Lane 1*, control cells; *lane 2*, 3-h incubation with C2IN-C3/C2II; *lane 3*, 3-h incubation with C2IN-C3/C2II followed by a 6-h incubation in fresh medium; *lane 4*, control cells incubated for 9 h with cycloheximide; *lane 5*, 3-h incubation with C2IN-C3/C2II followed by a 6-h incubation in fresh medium and cycloheximide; *lane 6*, control cells incubated for 9 h with puromycin; *lane 7*, 3-h incubation with C2IN-C3/C2II followed by a 6-h incubation in fresh medium and puromycin. ADP-ribosylated RhoA is indicated by an *asterisk*.

RhoA protein is due to ongoing protein synthesis.

C3-induced Destruction of the Actin Cytoskeleton Is Prevented and Rapidly Reversed by CNF1—Because a small amount of newly synthesized RhoA protein appeared to induce the complete reassembly of actin filaments and reconstitution of the cellular morphology, we tested whether this process could be enhanced by incubation of C3-treated cells with the *E. coli* cytotoxic necrotizing factor, CNF1, which activates Rho by deamidation (16, 18). Therefore, actin stress fibers of CHO cells were destroyed by treatment (3 h) with the C3 fusion toxin (Fig. 7). The cells were subsequently incubated for 2 h with CNF1 in the presence of the C3 fusion toxin. Surprisingly, the cells started to form actin stress fibers as early as 60 min after CNF1 addition. The CNF1-induced rearrangement of the actin cytoskeleton was accompanied by a total reconstitution of "normal" cell morphology within about 2 h. CNF1 completely prevented the C3-induced breakdown of actin filaments when CNF was added 3 h prior to C2IN-C3 fusion toxin (data not shown). When both toxins were added together at the same time, a weak C3-induced disassembly of actin filaments was observed after 60 min. This effect was completely reversed by CNF1

within another 60 min. The same rapid recovery of actin stress fibers was observed when NIH 3T3 fibroblasts were exposed to the various toxin combinations (data not shown).

C3-induced ADP-ribosylation of Rho in the Presence of CNF1—Next we analyzed the extent of ADP-ribosylation of Rho after CNF1 treatment. As shown in Fig. 8, in C3-treated cells RhoA remained completely ADP-ribosylated even after treatment of cells with CNF1 for 3 h (*lane 4*) (note that at this time point all cells exhibited complete recovery of the actin cytoskeleton). Additionally, when C2IN-C3 and CNF1 were added together, RhoA was ADP-ribosylated (*lane 5*). After 3 h, the cells showed no disassembly of stress fibers or C3-typical cytopathic effects on cell morphology. Finally, preincubation of cells with CNF1 for 3 h did not prevent C3-induced ADP-ribosylation. Similar results were obtained with NIH 3T3 cells (data not shown).

The effects of CNF1 on the C3-induced alteration of cellular morphology occurred very rapidly, suggesting that the recovery of cell morphology was not caused by neosynthesis of Rho. However, to exclude that CNF1 accelerated the expression of Rho and to rule out that a very small amount of neosynthesized RhoA was sufficient for rebuilding of the actin cytoskeleton, we tested the toxin in combination with inhibitors of protein synthesis. Therefore, CHO cells were treated for 16 h with the C3 fusion toxin in the presence of cycloheximide. Subsequently, the cells were incubated with CNF1 for another 2 h in the presence of cycloheximide. Thereafter, cells were lysed and Rho was [^{32}P]ADP-ribosylated by C3. Fig. 9*A* shows that no radioactive labeling of Rho was detected in lysates of cells pretreated with C3 or C3 plus CNF1. In contrast, pretreatment of cells with CNF1 did not inhibit the radiolabeling of Rho. These findings indicated that Rho from cells treated with fusion toxin and additionally with CNF1 was completely ADP-ribosylated. The anti-RhoA immunoblot (Fig. 9*B*) confirmed the ADP-ribosylation of RhoA and showed an additional shift of Rho due to CNF1-induced modification. Taken together, these results demonstrated that, despite the ADP-ribosylation of cellular Rho, CNF1 treatment causes complete and rapid reorganization of the actin cytoskeleton, even under conditions excluding the *de novo* synthesis of Rho.

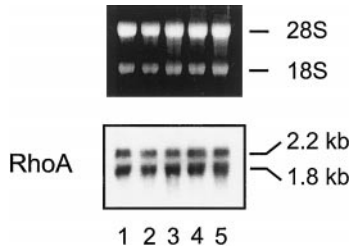

FIG. 6. **Northern blot analysis of RhoA mRNA in cultured CHO cells after C2IN-C3/C2II treatment and subsequent removal of the toxin.** Cells were treated with 100 ng/ml C2IN-C3 and 200 ng/ml C2II. After 3 h, cells were washed and incubated in fresh medium without toxin for the indicated times. The *upper panel* shows the 28 and 18 S ribosomal bands stained with ethidium bromide. The *lower panel* shows hybridization signals of RhoA (2.2 + 1.8 kilobases) mRNA. *Lane 1*, control cells; *lane 2*, 3-h incubation with C2IN-C3/C2II; *lane 3*, 5-h incubation with C2IN-C3/C2II; *lane 4*, 3-h incubation with C2IN-C3/C2II followed by a incubation for 3 h in fresh medium; *lane 5*, 3-h incubation with C2IN-C3/C2II followed by a incubation for 5 h in fresh medium.

Effect of ADP-ribosylation on Nucleotide Exchange of RhoA Activated by the Exchange Factor LBC—The results described above (*e.g.* activation of ADP-ribosylated Rho by CNF1) suggested that inhibition of Rho function by ADP-ribosylation is not caused by a blockade of the interaction of the GTPase with its effectors but rather by inhibition of its activation. To test this hypothesis, we studied the nucleotide release of ADP-ribosylated Rho previously loaded with mant-GDP in the presence of the Rho-specific nucleotide exchange factor LBC (30). As shown in Fig. 10*A*, the release of mant-GDP of control RhoA was stimulated by GST-LBC by about 13-fold, whereas LBC stimulated the release of the nucleotide from ADP-ribosylated Rho only by about 1.5-fold. This dramatic reduction in the activation of GDP release was observed over a broad concentration range of LBC (Fig. 10*B*).

DISCUSSION

To study kinetics and functional consequences of Rho ADP-ribosylation in intact cells, we used the C2IN-C3 fusion toxin that uses the cell delivery system of the binary *C. botulinum* C2 toxin to enter target cells (25). C2IN-C3 caused rapid disassembly of stress fibers and major changes in morphology in cultured rat astroglial cells and in CHO cells. The effects started within 40 min and were maximal about 2 h after toxin addition. As reported for the effects of the C3 exoenzyme (38, 39), these changes in morphology were preceded by a complete ADP-ribosylation of Rho. Surprisingly, the cells recovered within a few hours after removal of the toxin from the medium. Apparently, this recovery of the normal cell morphology depended on the occurrence of non-ADP-ribosylated RhoA. Concomitantly with the start of the rebuilding of stress fibers, a small amount of non-ADP-ribosylated RhoA was detected. Twenty-four hours after toxin removal, when reconstitution of

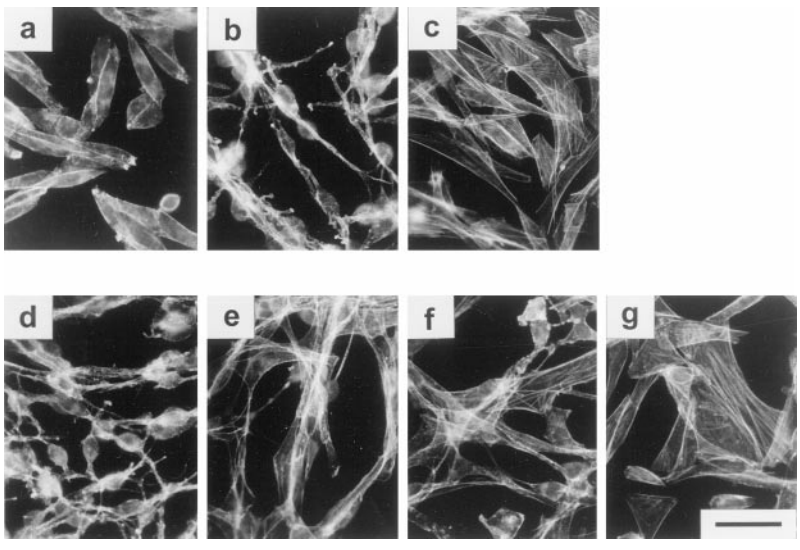

FIG. 7. **Disassembly of actin filaments induced by C2IN-C3 is rapidly reversed in CHO cells by CNF1.** Cells were treated for 3 h with 100 ng/ml C2IN-C3 and 200 ng/ml C2II at 37 °C (*b*). Then GST-CNF1 (300 ng/ml) was added and the cells were further incubated. After 30 min (*d*), 60 min (*e*), 90 min (*f*), and 120 min (*g*), the cells were fixed and stained with rhodamine-phalloidin. For controls, cells without toxin (*a*) and cells treated for 2 h with GST-CNF1 (*c*) were used. Cells were fixed, and actin filaments of respective cells were stained with rhodamine phalloidin. *Bar* = 50 μm.

the actin cytoskeleton and regeneration of cellular morphology were complete, only non-ADP-ribosylated Rho was observed. Subsequently, we tested whether reappearance of non-ADP-ribosylated Rho result from cleavage of the ADP-ribose moiety of modified Rho or from *de novo* synthesis of the GTPase. Cleavage of arginine-linked ADP-ribose is catalyzed by specific ADP-ribosylarginine hydrolases (40), but ADP-ribosylasparagine hydrolase has not been identified so far. Moreover, we were not able to obtain any evidence for a cleavage of the ADP-ribose moiety attached to Rho by hydrolase activity. In contrast, the translation inhibitors cycloheximide and puromycin blocked *de novo* synthesis of RhoA and prevented the recovery of cell morphology. This finding strongly suggested that Rho neosynthesis is crucial for reversal of cell morphology. Since Northern blot analysis did not show an increase in RhoA mRNA after treatment with C2IN-C3 or after its removal, the rapid *de novo* synthesis of RhoA was not due to enhanced transcription. Therefore, we conclude that the constitutive biosynthesis of RhoA is sufficient to restore RhoA functions. Morphological changes were reversed when neosynthesis had provided at approximately 10% of the normal cellular content of Rho but when ADP-ribosylated Rho was still present. Thus, our findings do not support a dominant negative role of ADP-ribosylated Rho as suggested from microinjection studies (39). This discrepancy may be explained by the high protein concentration usually used in such microinjection studies.

In addition to rapid neosynthesis of RhoA, the recovery of normal cell morphology depended on the intracellular degradation of the toxin. Since addition of the proteasome inhibitor lactacystin prevented the recovery of the normal cell morphology, the C2IN-C3 fusion toxin was probably degraded by the proteosomal pathway (41). Similarly, toxin degradation by the proteosomal pathway has been recently described for a fusion

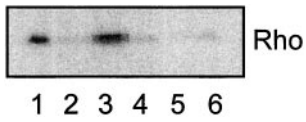

FIG. 8. **Influence of CNF1 on ADP-ribosylated Rho.** CHO cells were treated with the indicated combinations of C2IN-C3 (100 ng/ml)/C2II (200 ng/ml) and GST-CNF1 (300 ng/ml), lysed, and subjected to [^{32}P]ADP-ribosylation by C3 transferase. Autoradiogram of [^{32}P]ADP-ribosylation assay: *lane 1*, control cells; *lane 2*, cells incubated for 3 h with C2IN-C3 + C2II; *lane 3*, cells incubated for 3 h with CNF1; *lane 4*, cells incubated for 3 h with C2IN-C3 + C2II and subsequently for 3 h with CNF1; *lane 5*, cells incubated for 3 h with with C2IN-C3 + C2II together with CNF1; *lane 6*, cells incubated for 3 h with CNF1 and subsequently for 3 h with C2IN-C3 + C2II.

FIG. 9. **Analysis of ADP-ribosylation of Rho in CHO cells after treatment with C2IN-C3/C2II and CNF1.** Cells were treated for 16 h with 100 ng/ml C2IN-C3 and 200 ng/ml C2II at 37 °C in the presence of 20 μM cycloheximide. Then GST-CNF1 (300 ng/ml) was added for another 2 h in the presence of cycloheximide. The cells were lysed, and aliquots (50 μg protein) were [^{32}P]ADP-ribosylated by C3 transferase and analyzed by anti-RhoA immunoblot. *A*, autoradiography of [^{32}P]ADP-ribosylated Rho. *B*, anti-RhoA immunoblot. *Lane 1*, control cells; *lane 2*, 16-h incubation with C2IN-C3/C2II + 20 μM cycloheximide; *lane 3*, 2-h incubation with CNF1 (in the presence of cycloheximide); *lane 4*, 6-h incubation with C2IN-C3/C2II followed by 2-h incubation with CNF1 (in the presence of C2IN-C3/C2II and cycloheximide). RhoA, which is ADP-ribosylated and deamidated, is indicated by a *double asterisk*.

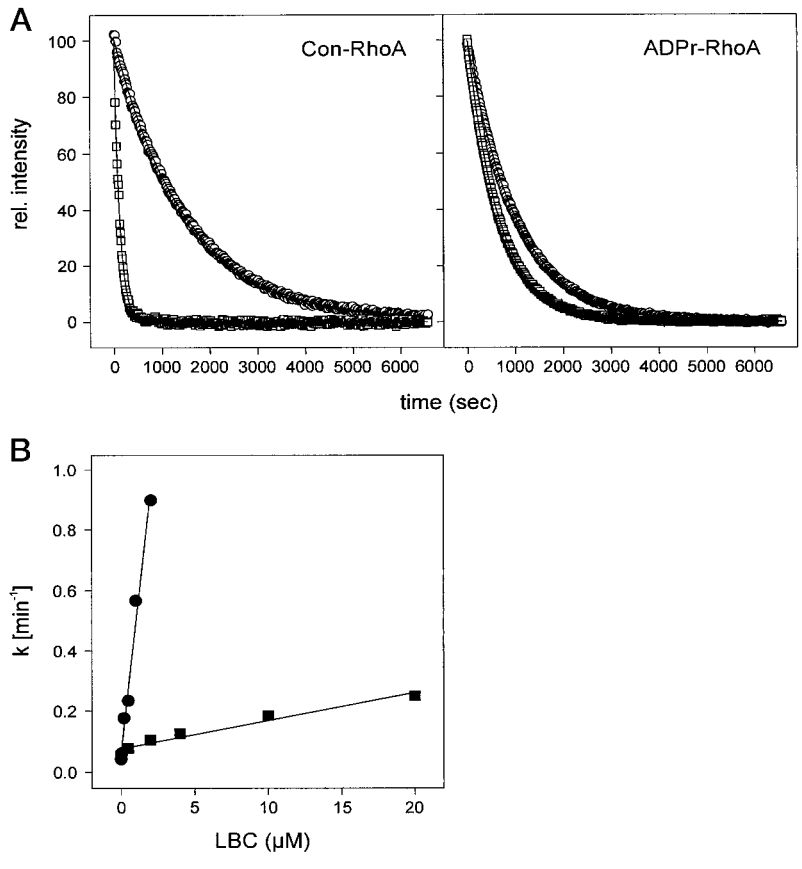

FIG. 10. **Influence of ADP-ribosylation on nucleotide release of RhoA stimulated by the nucleotide exchange factor LBC.** *A*, control RhoA (*Con-RhoA*, 0.5 μM) and ADP-ribosylated RhoA (*ADPr-RhoA*, 0.5 μM) were preloaded with mant-GDP and incubated at 37 °C. Release of the bound mant-GDP was started by the addition of 100 μM GTP in the absence (○) or presence of 1 μM GST-LBC (□). Nucleotide exchange was monitored by the decrease in the fluorescence of mant-GDP at 444 nm. Exciting of the mant-fluorophor was at 357 nm. *B*, plot of the rate constants for release of mant-GDP of control RhoA (●) and of ADP-ribosylated RhoA (■) determined at the indicated concentrations of LBC.

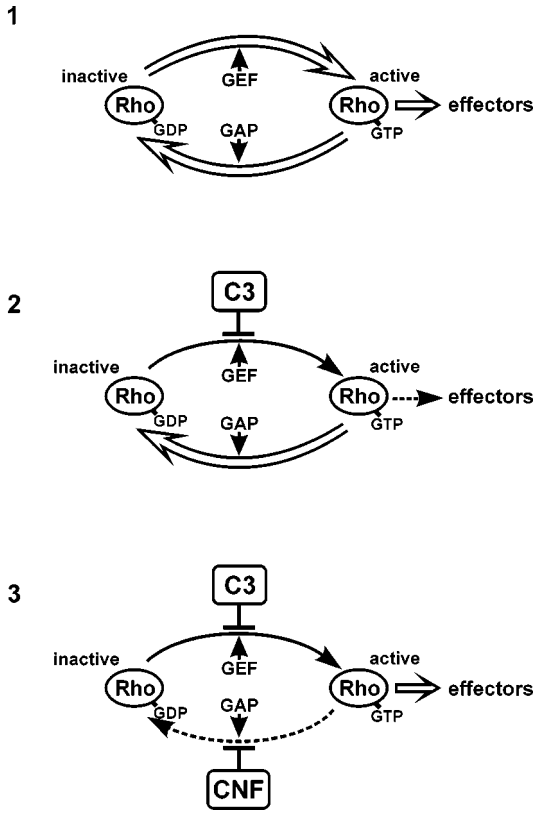

FIG. 11. **Effects of ADP-ribosylation and deamidation on the GTPase cycle of Rho.** *1*, inactive GDP-bound Rho is activated by nucleotide exchange, which is facilitated by guanine nucleotide exchange factors (*GEF*). The active GTP-bound state is terminated by hydrolysis of GTP, a process that is largely accelerated by GTPase-activating proteins (*GAP*). *2*, ADP-ribosylation of Rho inhibits the activation of Rho, while the off-reaction (GTP hydrolysis) is not inhibited. Therefore, the active species of Rho cannot accumulate. *3*, CNF1 deamidates and thereby blocks the inactivation of Rho. Although Rho is ADP-ribosylated, the active species accumulates and interacts with effectors to induce downstream responses.

protein of anthrax toxin, which is related to C2 toxin (42). In the presence of lactacystin only ADP-ribosylated Rho was detected, indicating that the ADP-ribosylating activity persisted in the cytosol and immediately modified the neosynthesized Rho. The data suggested that a continuous delivery of the toxin into the cytosol occurs in the presence of extracellular C2IN-C3. Consequently, the ADP-ribosylation of RhoA persists as long as the toxin is supplied. In contrast, cells treated with the *C. limosum* C3 exoenzyme did not recover within 24 h after removal of the toxin (data not shown). This difference in cell recovery may be explained by the different structures of the toxins and/or by the different modes and extent of cellular uptake.

In addition, *E. coli* cytotoxic necrotizing factor CNF1 reversed the morphological changes induced by C2IN-C3. CNF1 catalyzes the deamidation of glutamine at position 63 of Rho (16, 18). This modification blocks the GTPase activity of Rho and renders Rho constitutively active. The recovery of the flat cell morphology after removal of C2IN-C3 occurred much more rapidly in the presence than in the absence of CNF1. Surprisingly, recovery of the cell morphology and formation of stress fibers were induced by CNF1 even in the presence of C2IN-C3. Moreover analysis of Rho from cells treated in parallel with both toxins (*e.g.* CNF1 and C2IN-C3) revealed complete ADP-ribosylation of the GTPase. Thus, CNF1 was able to restore stress fiber formation despite the complete ADP-ribosylation of Rho. Recently, it has been described in Hep-2 cells that CNF1 prevented the cytopathic effects of C3B, a C3 fusion toxin consisting of C3 and the binding/translocation domain of diphtheria toxin (43). In this report it was suggested that CNF1 prevents ADP-ribosylation of Rho by C3 (43). In contrast, our data indicate that ADP-ribosylation and deamidation of Rho by CNF1 and C3, respectively, occur in parallel, but the functional consequences induced by CNF1 appear to be dominant. In addition to Rho, CNF1 was shown to deamidate and to activate Rac and Cdc42 (17). Also these GTPases are involved in organization of the actin cytoskeleton. However, there is no evidence that Rac and Cdc42 can substitute for Rho as regards the formation of stress fibers (2, 3). Therefore, our findings suggest that CNF1 induced the formation of an activated form of ADP-ribosylated Rho, which still interacted with cellular targets and was capable of activating effectors necessary for the formation of stress fibers and focal adhesions.

Moreover, this observation provides new insights into the molecular mechanism underlying the inactivation of Rho by ADP-ribosylation. It was shown that ADP-ribosylation has no major effects on nucleotide binding as well as hydrolysis of bound GTP. GAP-stimulated GTPase activity is not affected either (39, 44). Because the ADP-ribosylation at Asn^{41} occurs near the effector region of Rho, it has been suggested that the ADP-ribosylation blocks the interaction of Rho with its effectors (22). However, this hypothesis was not supported by findings that ADP-ribosylated Rho interacts with effectors like protein kinase N (44) or phosphatidyl-4-phosphate 5-kinase (45). Based on the observation that ADP-ribosylated Rho binds with even higher affinity to phosphatidyl-4-phosphate 5-kinase than the native RhoA, it was speculated that the effector activation step but not the binding is blocked by ADP-ribosylation (45). Our findings suggested that rather the activation step of Rho is crucially altered by ADP-ribosylation. This hypothesis was supported by the *in vitro* studies with recombinant ADP-ribosylated RhoA, showing that the stimulation of the GDP release from Rho by the guanine nucleotide exchange factor LBC was inhibited after ADP-ribosylation. Because the inactivation mechanism of ADP-ribosylated Rho by GTP hydrolysis is fully functional, a blocked or diminished activation of Rho will shift the GTPase to its inactive state (Fig. 11). Thus, after inhibition of the GTPase activity of Rho by CNF1, ADP-ribosylated Rho becomes active because the equilibrium between the inactive and active state is again shifted to the active state (Fig. 11).

Acknowledgments—We gratefully acknowledge the excellent technical assistance of Ulrike Müller and Brigitte Neufang.

REFERENCES

1. Hall, A. (1998) *Science* **279,** 509–514
2. Ridley, A. J., and Hall, A. (1992) *Cell* **70,** 389–399
3. Ridley, A. J., Paterson, H. F., Johnston, C. L., Diekmann, D., and Hall, A. (1992) *Cell* **70,** 401–410
4. Nobes, C. D., and Hall, A. (1995) *Cell* **81,** 53–62
5. Zeeuwen, P. L. J. M., Hendriks, W., de Jong, W. W., and Schalkwijk, J. (1997) *J. Biol. Chem.* **272,** 20471–20478
6. Prepens, U., Just, I., Von Eichel-Streiber, C., and Aktories, K. (1996) *J. Biol. Chem.* **271,** 7324–7329
7. Caron, E., and Hall, A. (1998) *Science* **282,** 1717–1721
8. Lamaze, C., Chuang, T. H., Terlecky, L. J., Bokoch, G. M., and Schmid, S. L. (1996) *Nature* **382,** 177–179
9. Schmalzing, G., Richter, H. P., Hansen, A., Schwarz, W., Just, I., and Aktories, K. (1995) *J. Cell Biol.* **130,** 1319–1332
10. Olson, M. F., Ashworth, A., and Hall, A. (1995) *Science* **269,** 1270–1272
11. Reuner, K. H., Wiederhold, M., Dunker, P., Just, I., Bohle, R. M., Kröger, M., and Katz, N. (1995) *Eur. J. Biochem.* **230,** 32–37
12. Khosravi-Far, R., Solski, P. A., Clark, G. J., Kinch, M. S., and Der, C. J. (1995) *Mol. Cell. Biol.* **15,** 6443–6453
13. Aktories, K. (1997) *Trends Microbiol.* **5,** 282–288
14. Just, I., Selzer, J., Wilm, M., Von Eichel-Streiber, C., Mann, M., and Aktories, K. (1995) *Nature* **375,** 500–503
15. Just, I., Wilm, M., Selzer, J., Rex, G., Von Eichel-Streiber, C., Mann, M., and Aktories, K. (1995) *J. Biol. Chem.* **270,** 13932–13936
16. Schmidt, G., Sehr, P., Wilm, M., Selzer, J., Mann, M., and Aktories, K. (1997) *Nature* **387,** 725–729

17. Lerm, M., Selzer, J., Hoffmeyer, A., Rapp, U. R., Aktories, K., and Schmidt, G. (1998) *Infect. Immun.* **67,** 496–503
18. Flatau, G., Lemichez, E., Gauthier, M., Chardin, P., Paris, S., Fiorentini, C., and Boquet, P. (1997) *Nature* **387,** 729–733
19. Braun, U., Habermann, B., Just, I., Aktories, K., and Vandekerckhove, J. (1989) *FEBS Lett.* **243,** 70–76
20. Aktories, K., Braun, U., Rösener, S., Just, I., and Hall, A. (1989) *Biochem. Biophys. Res. Commun.* **158,** 209–213
21. Chardin, P., Boquet, P., Madaule, P., Popoff, M. R., Rubin, E. J., and Gill, D. M. (1989) *EMBO J.* **8,** 1087–1092
22. Sekine, A., Fujiwara, M., and Narumiya, S. (1989) *J. Biol. Chem.* **264,** 8602–8605
23. Aktories, K., and Just, I. (1995) *Methods Enzymol.* **256,** 184–195
24. Aktories, K., Mohr, C., and Koch, G. (1992) *Curr. Top. Microbiol. Immunol.* **175,** 115–131
25. Barth, H., Hofmann, F., Olenik, C., Just, I., and Aktories, K. (1998) *Infect. Immun.* **66,** 1364–1369
26. Ohishi, I., Iwasaki, M., and Sakaguchi, G. (1980) *Infect. Immun.* **30,** 668–673
27. Aktories, K., and Wegner, A. (1989) *J. Cell Biol.* **109,** 1385–1387
28. Aktories, K., Bärmann, M., Ohishi, I., Tsuyama, S., Jakobs, K. H., and Habermann, E. (1986) *Nature* **322,** 390–392
29. Ohishi, I. (1987) *Infect. Immun.* **55,** 1461–1465
30. Zheng, Y., Olson, M. F., Hall, A., Cerione, R. A., and Toksoz, D. (1995) *J. Biol. Chem.* **270,** 9031–9034
31. Hiratsuka, T. (1983) *Biochim. Biophys. Acta* **742,** 496–508
32. Keller, M., Jackisch, R., Seregi, A., and Hertting, G. (1985) *Neurochem. Int.* **7,** 655–665
33. Hildebrand, B., Olenik, C., Uhl, A., and Meyer, D. K. (1997) *Brain Res.* **759,** 285–291
34. Laemmli, U. K. (1970) *Nature* **227,** 680–685
35. Cheley, S., and Anderson, R. (1984) *Anal. Biochem.* **137,** 15–19
36. Olenik, C., Barth, H., Just, I., Aktories, K., and Meyer, D. K. (1997) *Mol. Brain Res.* **52,** 263–269
37. Höltke, H.-J., and Kessler, C. (1990) *Nucleic Acids Res.* **18,** 5843–5851
38. Wiegers, W., Just, I., Müller, H., Hellwig, A., Traub, P., and Aktories, K. (1991) *Eur. J. Cell Biol.* **54,** 237–245
39. Paterson, H. F., Self, A. J., Garrett, M. D., Just, I., Aktories, K., and Hall, A. (1990) *J. Cell Biol.* **111,** 1001–1007
40. Takada, T., Iida, K., and Moss, J. (1993) *J. Biol. Chem.* **268,** 17837–17843
41. Fenteany, G., and Schreiber, S. (1998) *J. Biol. Chem.* **273,** 8545–8548
42. Goletz, T. J., Klimpel, K. R., Arora, N., Leppla, S. H., Keith, J. M., and Berzofsky, J. A. (1997) *Proc. Natl. Acad. Sci. U. S. A.* **94,** 12059–12064
43. Fiorentini, C., Donelli, G., Matarrese, P., Fabbri, A., Paradisi, S., and Boquet, P. (1995) *Infect. Immun.* **63,** 3936–3944
44. Sehr, P., Joseph, G., Genth, H., Just, I., Pick, E., and Aktories, K. (1998) *Biochemistry* **37,** 5296–5304
45. Ren, X.-D., Bokoch, G. M., Traynor-Kaplan, A., Jenkins, G. H., Anderson, R. A., and Schwartz, M. A. (1996) *Mol. Biol. Cell* **7,** 435–442